

V.F. Bolyukh, A.I. Kocherga, I.S. Schukin

ELECTROMECHANICAL PROCESSES IN A LINEAR PULSE-INDUCTION ELECTROMECHANICAL CONVERTER WITH A MOVABLE INDUCTOR AND TWO ARMATURES

Purpose. The purpose of the paper is to determine the influence of the height of the mobile and stationary disk electrically conductive armatures covering the movable inductor on the electromechanical processes of linear pulsed-induction electromechanical converter (LPIEC). *Methodology.* With the help of the developed mathematical model that describes electromechanical and thermal processes of LPIEC, the influence of the heights of the armatures on electromechanical processes, the values of the electrodynamic forces acting on the inductor and armature, and the moving speed of the movable armature (MA) is established. *Results.* It is shown that if the height of the stationary armature (SA) is twice the height of the MA, then the inductor at the initial instant of time is acted upon by electrodynamic forces pressing it to the SA, and the displacement of the inductor begins with a delay of 0.35 ms. If the height of the MA is twice the height of the SA, then the electrodynamic forces act on the inductor at the initial instant of time, repelling it from the SA, and its movement begins with a delay of 0.1 ms. If the heights of the SA and the MA are equal, then until the time 0.15 ms on the inductor, the electrodynamic forces practically do not act and the inductor moving relative to the SA begins with a delay of 0.25 ms. *Originality.* The effect of the geometric parameters of the SA and MA on the velocity of the inductor moving relative to the SA, MA relative to the inductor and the MA relative to the SA is established. It has been established that the highest velocity of the MA relative to the SA develops the lowest MA, and the height of the SA does not affect it practically. However, with the increase in the height of the MA, the effect of SA begins to affect. In this case, it is expedient to select the height of the SA to be 0.4-0.42 of the height of the inductor. *Practical value.* It is shown that as the weight of the actuating element increases, the currents in the active elements of the LPIEC increase, the induction velocities of the inductor relative to the SA and the MA decrease relative to the inductor. At the same time, the maximum the electrodynamic forces values acting on the inductor decrease, and the armatures increase. Moreover, the maximum the electrodynamic forces acting on the MA are less than similar forces acting on the SA. References 12, figures 7.

Key words: linear pulse-induction electromechanical converter, mathematical model, mobile inductor, stationary armature, movable armature, electromechanical processes.

Разработана математическую модель, которая описывает электромеханические процессы в линейном импульсно-индукционном электромеханическом преобразователе с подвижным индуктором, взаимодействующим со стационарным якорем (СЯ) и подвижным якорем (ПЯ), ускоряющим исполнительный элемент. Установлено влияние высот якорей на электромеханические процессы в преобразователе. Если высота СЯ в два раза больше высоты ПЯ, то на индуктор в начальный момент времени действуют электродинамические усилия (ЭДУ), прижимающие его к СЯ и перемещение индуктора начинается с задержкой 0,35 мс. Если высота ПЯ в два раза больше высоты СЯ, то на индуктор в начальный момент времени действуют ЭДУ, отталкивающие его от СЯ, и его перемещение начинается с задержкой 0,1 мс. Если высоты СЯ и ПЯ равны, то до момента времени 0,15 мс на индуктор практически не действуют ЭДУ и перемещение индуктора начинается с задержкой 0,25 мс. Установлены комбинации геометрических параметров якорей, при которых действуют как наибольшие, так и наименьшие импульсы ЭДУ. Наибольшие скорости развивает наиболее низкий ПЯ, причем высота СЯ на них практически не влияет. С увеличением массы исполнительного элемента происходит увеличение токов в активных элементах преобразователя и уменьшение скоростей индуктора и ПЯ. При этом максимальные значения ЭДУ, действующих на индуктор, уменьшаются, а на якоря – увеличиваются. Библ. 12, рис. 7.

Ключевые слова: линейный импульсно-индукционный электромеханический преобразователь, математическая модель, подвижный индуктор, стационарный якорь, подвижный якоря, электромеханические процессы.

Introduction. Linear pulsed electromechanical converters are designed to provide high speed of the actuating element (AE) on a short active section, and/or to create shock force pulses [1-4]. Such converters are used in many branches of science and technology as electromechanical accelerators and shock-power devices [5-7]. The most widely used are linear pulse-induction electromechanical converters (LPIEC) of a coaxial configuration in which the accelerated electrically conductive armature interacts non-contact with a stationary inductor [1, 2, 8]. At excitation of a multi-turn inductor from capacitive energy storage (CES) in an electrically conductive armature made in the form of a copper disk, eddy currents are induced. As a result, the electrodynamic forces (EDF) of the repulsion act on the armature, causing its axial movement together with the AE relative to the inductor.

However, when operating in a dynamic mode with a rapid change in the electromagnetic, mechanical, and thermal parameters, the force and speed indicators of the LPIEC of traditional design are not high enough [9]. One of the ways to increase these indicators is the development of new design schemes of the LPIEC [10, 11]. Since in the traditional LPIEC design with an armature only one side of the inductor interacts inductively, a significant part of the magnetic field from the opposite side of the inductor is scattered into the surrounding space, negatively affecting closely located electronic and biological objects and is not used to create additional EDF.

Let us consider a constructive scheme of a LPIEC of a coaxial configuration, containing a movable inductor, enveloped on opposite sides by two electrically

conductive armatures (Fig. 1). One of the armatures interacts with the fixed stop, and the second one interacts with an actuating element, for example, of a shock-power device.

When the inductor is excited through flexible or sliding contacts from the CES C , the EDF of repulsion occur between the inductor and the armature, which leads to the movement of the movable armature (MA) relative to the inductor, which in turn repels with respect to the stationary armature (SA). This raises the question of the effect of geometric parameters of armatures on electromechanical processes in LPIEC. Since the radial dimensions of the armatures, as a rule, correspond to the radial dimensions of the inductor, the question arises as to the effect of the axial dimensions of the electrically conductive armatures on the force and speed indicators of the LPIEC.

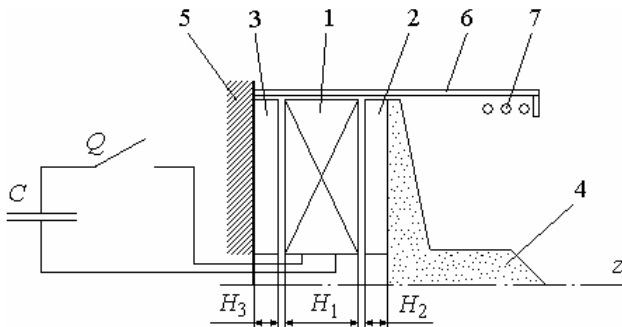


Fig. 1. Constructive scheme of the LPIEC: 1 – inductor; 2 – stationary armature; 3 – movable armature; 4 – actuating element; 5 – stop; 6 – case; 7 – damper spring

The goal of the paper is determination of the influence of the height of the mobile and stationary disk armatures covering the movable inductor on electromechanical processes in the LPIEC.

Mathematical model. Consider a mathematical model that describes electromechanical processes in LPIEC using lumped parameters of active elements – inductor, stationary and mobile armatures:

$$i_1 R_1(T_1) + L_1 \frac{di_1}{dt} + \frac{1}{C} \int i_1 dt + M_{12}(z) \frac{di_2}{dt} + M_{13}(z) \frac{di_3}{dt} + v_{12}(t) i_2 \frac{dM_{12}}{dz} + v_{13}(t) i_3 \frac{dM_{13}}{dz} = 0; \quad \frac{1}{C} \int i_1 dt = U_0; \quad (1)$$

$$i_2 R_2(T_2) + L_2 \frac{di_2}{dt} + M_{12}(z) \frac{di_1}{dt} + M_{23}(z) \frac{di_3}{dt} + i_1 \xi_1 + i_3 \xi_3 = 0; \quad (2)$$

$$i_3 R_3(T_3) + L_3 \frac{di_3}{dt} + M_{13}(z) \frac{di_1}{dt} + M_{23}(z) \frac{di_2}{dt} + i_1 \xi_2 + i_2 \xi_3 = 0; \quad (3)$$

$$i_1 i_3 \frac{dM_{13}}{dz} = i_1 i_2 \frac{dM_{12}}{dz} + (m_1 + m_2 + m_e) \frac{dv_{13}}{dt} + K_T v_{13}(t); \quad (4)$$

$$i_1 i_2 \frac{dM_{12}}{dz} = i_2 i_3 \frac{dM_{23}}{dz} + (m_2 + m_e) \frac{dv_{12}}{dt} + K_T \cdot (v_{13}(t) + v_{12}(t)) + 0.125 \pi \gamma_a \beta_a D_{2m}^2 [v_{12}(t) + v_{13}(t)]^2 + K_P [\Delta z_{12}(t) + \Delta z_{13}(t)]; \quad (5)$$

where $\xi_1 = v_{12}(t) \frac{dM_{12}}{dz}$; $\xi_2 = v_{13}(t) \frac{dM_{13}}{dz}$; $p=1, 2, 3$ are the indexes of the inductor, MA and SA; $\xi_3 = (v_{12}(t) + v_{13}(t)) \frac{dM_{23}}{dz}$; $R_p(T_p)$, L_p , i_p are the resistance, inductance and current of the p -th active element,

respectively; $M_{12}(z)$, $M_{13}(z)$, $M_{23}(z)$ are the mutual inductances between corresponding p -th active elements; $v_{13}(t)$, $v_{12}(t)$ are the speeds of the inductor relative SA and MA along the z -axis, respectively; $\Delta z_{13}(t)$, $\Delta z_{12}(t)$ are the displacements of the inductor relative SA and of the MA relative inductor, respectively; m_1 , m_2 , m_e are the masses of the inductor, MA and actuating element, respectively.

The coupled solution of equations (1) – (3) allows us to reduce them to one differential equation:

$$a_4 \frac{d^4 i_1}{dt^4} + a_3 \frac{d^3 i_1}{dt^3} + a_2 \frac{d^2 i_1}{dt^2} + a_1 \frac{di_1}{dt} + a_0 = 0, \quad (6)$$

where $a_4 = L_1 b_1 + M_{13} d_2 + M_{12} d_3$;

$$a_3 = R_1 b_1 + R_2 b_2 + R_3 b_3 + 2(e_1 d_1 + e_2 d_2 + e_3 d_3);$$

$$a_2 = b_1 / C + L_1 (R_2 R_3 - e_1^2) + L_2 (R_1 R_3 - e_2^2) + L_3 (R_1 R_2 - e_3^2) + 2[M_{12}(e_1 e_2 - R_3 e_3) + M_{13}(e_1 e_3 - R_2 e_2) + M_{23}(e_2 e_3 - R_1 e_1)];$$

$$a_1 = R_1 (R_2 R_3 - e_1^2) + e_2 (e_1 e_3 - R_2 e_2) + e_3 (e_1 e_2 - R_3 e_3) + (R_2 L_3 + R_3 L_2 - 2M_{23} e_1) / C;$$

$$a_0 = (R_2 R_3 - e_1^2) / C; \quad b_1 = L_2 L_3 - M_{23}^2; \quad b_2 = L_1 L_3 - M_{13}^2;$$

$$b_3 = L_1 L_2 - M_{12}^2; \quad d_1 = M_{12} M_{13} - L_1 M_{23};$$

$$d_2 = M_{12} M_{23} - L_2 M_{13}; \quad d_3 = M_{13} M_{23} - L_3 M_{12};$$

$$e_1 = (v_{13} + v_{12}) \frac{dM_{23}}{dz}; \quad e_2 = v_{13} \frac{dM_{13}}{dz}; \quad e_3 = v_{12} \frac{dM_{12}}{dz}.$$

The characteristic equation of the differential equation (6)

$$a_4 x^4 + a_3 x^3 + a_2 x^2 + a_1 x + a_0 = 0 \quad (7)$$

by means of a substitution $\varpi = x + 0.25a_3/a_4$ is transformed into the reduced form with a cubic resolvent:

$$\varpi^3 + q_1 \cdot \varpi^2 + q_2 \cdot \varpi - q_3^2 = 0, \quad (8)$$

where $q_1 = 2 \frac{a_2}{a_4} - 0.75 \left(\frac{a_3}{a_4} \right)^2$;

$$q_2 = 3 \left(\frac{a_3}{2 \cdot a_4} \right)^4 - \frac{a_3^2 \cdot a_2}{a_4^3} + \frac{a_1 \cdot a_3 + a_2^2}{a_4^2} - 4 \frac{a_0}{a_4};$$

$$q_3 = \left(\frac{a_3}{2 \cdot a_4} \right)^3 - 0.5 \frac{a_2 \cdot a_3}{a_4^2} + \frac{a_1}{a_4}.$$

If the discriminant of the resolvent

$$D = (u/3)^3 - (v/2)^2, \quad (9)$$

where $u = q_2 - q_1^2/3$; $v = 2 \cdot q_1^3/27 - q_1 \cdot q_2/3 - q_3^2$,

is less than zero, then, using the trigonometric solution of equation (8), we obtain:

$$\varpi_p = 2 \cdot \sqrt[3]{\left(-\frac{u^3}{27}\right)^{0.5}} \cos \left(\frac{2\pi(p-1)}{3} + \frac{\arccos\left(-0.5v\sqrt{-27/a_3^3}\right)}{3} \right). \quad (10)$$

In this case, the roots of equation (7):

$$x_l = 0.5 \cdot (\pm \sqrt{\varpi_1} \pm \sqrt{\varpi_2} \pm \sqrt{\varpi_3}) - 0.25 \cdot a_3 / a_4, \quad (11)$$

where $l = 1, 2, 3, 4$.

If all the roots of (11) are real, then for the currents in the p -th active elements of the LPIEC we can write:

$$i_p = \frac{U_0 t}{a_4 \mathcal{G}}, \quad (12)$$

where

$$\begin{aligned} t &= A_{p1} \exp(x_1 t) + A_{p2} \exp(x_2 t) + A_{p3} \exp(x_3 t) + A_{p4} \exp(x_4 t) \\ g &= \gamma_{21} \gamma_{43} (\delta_{21} + \delta_{43}) + \gamma_{24} \gamma_{31} (\delta_{24} + \delta_{31}) + \gamma_{32} \gamma_{41} (\delta_{32} + \delta_{41}), \\ A_{p1} &= \gamma_{32} (\alpha_4 - \Theta_p \delta_{32}) + \gamma_{24} (\alpha_3 - \Theta_p \delta_{24}) + \gamma_{43} (\alpha_2 - \Theta_p \delta_{43}); \\ A_{p2} &= \gamma_{13} (\alpha_2 - \Theta_p \delta_{13}) + \gamma_{41} (\alpha_3 - \Theta_p \delta_{41}) + \gamma_{34} (\alpha_1 - \Theta_p \delta_{34}); \\ A_{p3} &= \gamma_{21} (\alpha_4 - \Theta_p \delta_{21}) + \gamma_{42} (\alpha_1 - \Theta_p \delta_{42}) + \gamma_{14} (\alpha_2 - \Theta_p \delta_{14}); \\ A_{p4} &= \gamma_{12} (\alpha_3 - \Theta_p \delta_{12}) + \gamma_{31} (\alpha_2 - \Theta_p \delta_{31}) + \gamma_{23} (\alpha_1 - \Theta_p \delta_{23}); \\ n &= 2, 3; \quad m = 5 - n; \end{aligned}$$

$$\gamma_{kl} = x_k - x_l; \quad \alpha_k = (\Lambda_p x_k - \Xi_p) x_k^2; \quad \delta_{kl} = x_k^2 x_l^2;$$

$$\Theta_1 = -b_1; \quad \Theta_n = -d_m; \quad \Lambda_1 = \zeta_1 / a_4; \quad \Lambda_n = \zeta_n / a_4;$$

$$\Xi_1 = [a_4 b_1^2 / C - \zeta_1 (R_1 b_1 + e_2 d_2 + e_3 d_3) - \zeta_2 (R_2 d_3 + e_3 b_1 + e_1 d_2) - \zeta_3 (R_3 d_2 + e_2 b_1 + e_1 d_3)] / a_4^2;$$

$$\Xi_n = [a_4 b_1 d_m / C - \zeta_1 (R_1 d_m + e_m b_n + e_n d_1) - \zeta_n (R_n b_n + e_m d_m + e_1 d_1) - \zeta_m (R_m d_1 + e_n d_m + e_1 b_n)] / a_4^2;$$

$$\zeta_1 = R_1 b_1^2 + R_2 d_3^2 + R_3 d_2^2 + 2[b_1 (e_2 d_2 + e_3 d_3) + e_1 d_2 d_3];$$

$$\zeta_n = d_m (R_1 b_1 + R_n b_n) + R_m d_1 d_n + e_m (b_1 b_n + d_m^2) - (e_n b_1 + e_1 d_m) \times L_1 M_{nm} - L_n M_{1m} (e_n d_m + e_1 b_n) - L_m M_{1n} (e_1 d_1 + e_n d_n).$$

If the discriminant of the resolvent (9) is greater than zero, then, using Cardano solution for equation (8), we obtain one real and two complex conjugate roots:

$$\omega_1 = \phi + \zeta - q_1 / 3; \quad \omega_{2,3} = \varepsilon \pm j\chi, \quad (13)$$

$$\text{where } \phi = \sqrt[3]{-0.5 \cdot v + \sqrt{D}}; \quad \zeta = \sqrt[3]{-0.5 \cdot v - \sqrt{D}};$$

$$\varepsilon = -0.5 \cdot (\phi + \zeta) - q_1 / 3; \quad \chi = 0.5 \cdot \sqrt{3} (\phi - \zeta).$$

In this case, the roots of equation (7) have the form:

$$x_{1,2} = 0.5 \cdot \sqrt{\omega_1} - 0.25 \cdot a_3 / a_4 \pm \sqrt{0.5 \cdot \left(\varepsilon + \sqrt{\varepsilon^2 + \chi^2} \right)};$$

$$x_{3,4} = \sigma \pm j\xi, \quad (14)$$

$$\text{where } \sigma = 0.5 \cdot \sqrt{\omega_1} - 0.25 \cdot a_3 / a_4;$$

$$\xi = \sqrt{0.5 \cdot \left(-\varepsilon + \sqrt{\varepsilon^2 + \chi^2} \right)}.$$

If x_1 and x_2 are real and different, the currents in the p -th active elements can be represented as:

$$i_p = \frac{U_0 \lambda}{a_4 \aleph}, \quad (15)$$

where

$$\aleph = x_1 x_2 (3\sigma^2 - 2\sigma x_1 - \xi^2 + x_1 x_2) + \chi_2 (\chi_2 + \chi_3 - 2\sigma x_1);$$

$$\lambda = B_{p1} \exp(x_1 t) + B_{p2} \exp(x_2 t) + \exp(\sigma \cdot t) [B_{p3} \cos(\xi t) + B_{p4} \sin(\xi t)];$$

$$B_{p1} = \left\{ \Theta_p \left[x_2^2 (3\sigma^2 - \xi^2 - 2x_2 \sigma) - \chi_2^2 \right] + \Lambda_p \left[2\sigma x_2 - x_2 (3\sigma^2 - \xi^2 - x_2^2) \right] - \Xi_p \left[(\sigma - x_2)^2 + \xi^2 \right] \right\} / (x_2 - \xi);$$

$$B_{p2} = \left\{ \Theta_p \left[x_2^2 + \sigma^2 (\xi^2 - 3\sigma^2 + 2x_1 \sigma) \right] + \Lambda_p \left[x_1 (3\sigma^2 - \xi^2) - 2\sigma x_2 \right] + \Xi_p (x_2 - 2x_1 \sigma) \right\} / (x_2 - \xi);$$

$$B_{p3} = \Theta_p \left[(\xi^2 - 3\sigma^2) \chi_1 + 2\sigma \chi_3 \right] + \Lambda_p \left[(3\sigma^2 - \xi^2) - \chi_3 \right] + \Xi_p (x_1 - 2\sigma);$$

$$B_{p4} = \left\{ \Theta_p \left[x_3 (\xi^2 - \sigma^2) + \chi_1 \sigma (\sigma^2 - 3\xi^2) + x_1^2 x_2^2 \right] + \Lambda_p (\chi_3 \sigma - x_1 x_2 \chi_1 + 3\sigma \xi^2 - \sigma^3) + \Xi_p \left(\sigma^2 - \xi^2 + x_1 x_2 - \sigma \xi \right) \right\} / \xi;$$

$$\chi_1 = x_1 + x_2; \quad \chi_2 = \sigma^2 + \xi^2; \quad \chi_3 = x_1^2 + x_1 x_2 + x_2^2.$$

The displacements of the inductor relative to the SA, as well as the MA relative to the inductor on the basis of equations (4) and (5) can be represented in the form of recurrence relations:

$$\begin{aligned} \Delta z_{13}(t_{k+1}) &= \left[i_1(t_k) \left(i_3(t_k) \frac{dM_{13}}{dz} - i_2(t_k) \frac{dM_{12}}{dz} \right) - K_T v_{13}(t_k) \right] \times \\ &\times 0.5 \frac{\Delta t^2}{m_1 + m_2 + m_e} + \Delta z_{13}(t_k) + v_{13}(t_k) \Delta t, \quad (16) \end{aligned}$$

$$\begin{aligned} \Delta z_{12}(t_{k+1}) &= \Delta z_{12}(t_k) + v_{12}(t_k) \Delta t + \frac{\Delta t^2}{2(m_2 + P)} \times \\ &\times \left[\left(i_1(t_k) \frac{dM_{12}}{dz} - i_3(t_k) \frac{dM_{23}}{dz} \right) i_2(t_k) - K_T (v_{12}(t_k) + v_{13}(t_k)) - \right. \\ &- 0.125 \cdot \pi \cdot \beta_a \gamma_a D_{2m}^2 [v_{12}(t_k) + v_{13}(t_k)]^2 - \\ &\left. - K_P (\Delta z_{12}(t_k) + \Delta z_{13}(t_k)) \right]. \quad (17) \end{aligned}$$

The temperature of the p -th active element at moving the armature and inductor, when there is no thermal contact between them, can be described by the recurrence relation [10]:

$$\begin{aligned} T_p(t_{k+1}) &= T_p(t_k) \chi + (1 - \chi) \left[T_0 + 4\pi^{-2} i_p(t_k) R_p(T_n) \alpha_{Tp}^{-1} \times \right. \\ &\times \left. D_{ep}^{-1} H_p^{-1} (D_{ep}^2 - D_{ip}^2)^{-1} \right], \quad (18) \end{aligned}$$

where $\chi = \exp\left\{-0.25 \Delta t D_{ep} \alpha_{Tp} c_p^{-1} (T_p) \gamma_p^{-1}\right\}$; D_{ep} , D_{ip} are the outer and inner diameters of the p -th active element, respectively; α_{Tp} is the heat transfer coefficient of the p -th active element; c_p is the heat capacity of the p -th active element.

The initial conditions of the system of equations (1) – (18): $T_p(0) = T_0$ is the temperature of the p -th active element; $i_p(0) = 0$ is the current of the p -th active element; $\Delta z(0) = 1$ mm is the initial axial distance between the armatures and the inductor; $u_c(0) = U_0$ is the voltage of the CES; $v_z(0) = 0$ is the armature speed along the z -axis.

In order to take into account the complex of interconnected electric, magnetic, thermal and mechanical processes and various nonlinear dependencies, the transient process is divided into a large number of time intervals $\Delta t = t_{k+1} - t_k$ within which all quantities are assumed to be unchanged. With such a numerical-analytical approach within a small interval Δt the previously defined analytical expressions are used to calculate the basic quantities, and the transient process is calculated using iterative relationships using computer.

LPIEC main parameters. Let us consider LPIEC of a coaxial configuration, in which both armatures are made in the form of a flat disc of technical copper, one of whose sides faces the inductor.

Inductor: outer diameter $D_{exi} = 100$ mm, inner diameter $D_{ini} = 10$ mm, height $H_1 = 10$ mm, copper bus section $a \times b = 1.8 \times 4.8$ mm², bus number of turns $N_1 = 46$. The inductor is made in the form of a double-layer winding with external electrical terminals.

Armatures: outer diameter $D_{ex2,3} = 100$ mm, inner diameter $D_{in2,3} = 10$ mm, height $H_2 = H_3 = 3 - 7$ mm.

CES: capacitance $C = 500 \mu\text{F}$, voltage $U_0 = 1.5 \text{ kV}$.

Actuating element has mass $m_e = 1 \text{ kg}$.

LPIEC electromechanical characteristics. We consider the influence of the height of armatures on electromechanical processes of the LPIEC. The height of the MA will be estimated by a dimensionless geometric parameter $h_2^* = H_2 H_1^{-1}$, and the height of the SA by a parameter $h_3^* = H_3 H_1^{-1}$.

Let us consider the electromechanical characteristics of the LPIEC having various combinations of the heights of the SA and the MA.

Fig. 2 shows the electromechanical characteristics of the LPIEC, in which the height of the SA is twice the height of the MA (armatures parameters $h_2^* = 0.3$, $h_3^* = 0.6$).

The current in the inductor with density j_1 has a vibrationally damped character. The maximum inductor current density is 554.6 A/mm^2 . At the initial moment of the operation process the current densities in the MA j_2 and in the SA j_3 have a polarity opposite to the inductor. The maximum current density in the MA is 554.6 A/mm^2 , and in the SA 303 A/mm^2 . Due to the interaction of currents, on the MA, electrodynamic forces of repulsion f_{z2} act with maximum value of 13.6 kN .

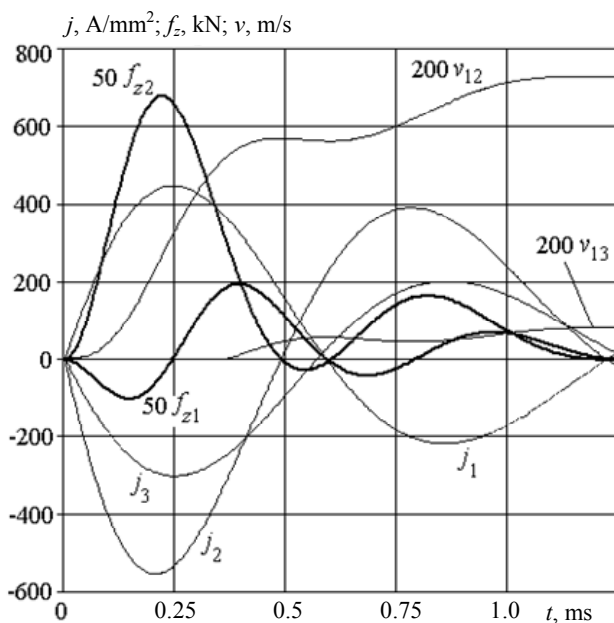


Fig. 2. Electromechanical characteristics of the LPIEC with armatures geometrical parameters $h_2^* = 0.3$, $h_3^* = 0.6$

In the interval 0.5-0.65 ms EDF change direction, after which a repetition of repulsive forces, but much less than in the original one, takes place. As a result, the MA moves relative to the inductor at a speed v_{12} the maximum value of which is 3.65 m/s .

On the inductor at the initial instant of time, negative EDFs f_{z1} act, pressing it to the SA. However, after 0.25 ms, these EDFs, changing the direction, repel the inductor from the SA with a maximum value of 3.9 kN . As a result, the inductor moves relative to the SA with a speed v_{13} the maximum value of which is 0.4 m/s . And the displacement of the inductor begins with a delay of 0.35 ms. The value of the maximum speed of the MA relative to the SA is 4.05 m/s .

Fig. 3 shows the electromechanical characteristics of the LPIEC, in which the height of the MA is twice the height of the SA (armatures parameters $h_2^* = 0.6$, $h_3^* = 0.3$).

In this LPIEC, as in the considered above, the character of the current flow is preserved. The maximum current density in the inductor j_1 slightly increases to 450.1 A/mm^2 . The maximum current density j_2 in the MA decreases to 294.3 A/mm^2 , and in SA j_3 the current density rises to 573 A/mm^2 . As a result, the maximum EDF of repulsion acting on f_{z2} decreases to 12.7 kN . As a result, the maximum speed of moving the MA relative to the inductor v_{12} decreases to 2.95 m/s .

However, in this LPIEC, positive EDF f_{z1} act on the inductor at the initial instant of time, repelling it from the SA and its movement begins in about 0.1 ms. The maximum value of these forces is observed in the second peak of repulsion, reaching 2.18 kN . As a result, the inductor moves relative to the SA with a velocity v_{13} , the maximum value of which reaches 0.63 m/s . The maximum speed of the MA relative to the SA v_{23} is 3.58 m/s . The decrease in the speed of the MA can be explained by its increased mass.

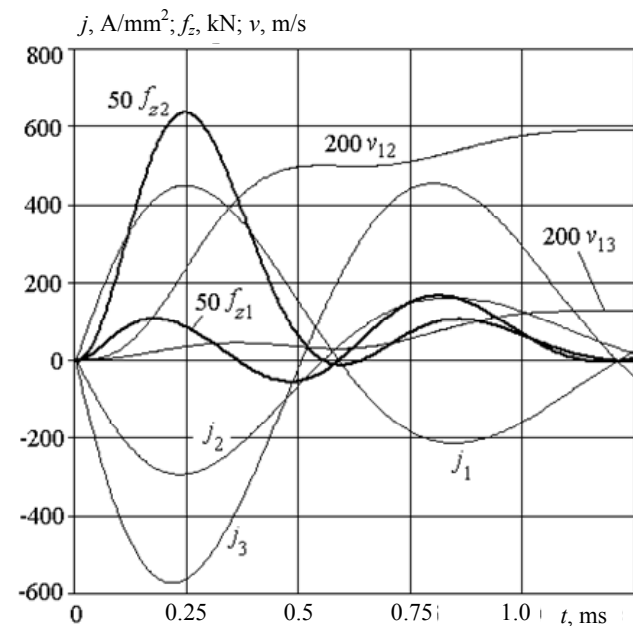


Fig. 3. Electromechanical characteristics of the LPIEC with armatures geometrical parameters $h_2^* = 0.6$, $h_3^* = 0.3$

Let us consider the LPIEC variant, in which the heights of the SA and the MA are equal. Fig. 4 presents the electromechanical characteristics of the LPIEC with parameters $h_2^* = 0.4$, $h_3^* = 0.4$.

In this LPIEC the maximum current density in the inductor j_1 is 442.8 A/mm^2 . The currents in the armatures, especially in the initial part of the process, where there is no movement of the active elements, are practically the same. The maximum current density j_2 in the MA is 420.3 A/mm^2 , and in the SA j_3 it is 434.8 A/mm^2 . The maximum EDF of repulsion acting on f_{z2} is 12.8 kN , which results in the displacement of the MA relative to the inductor at a speed of v_{12} , the maximum value of which is 3.28 m/s .

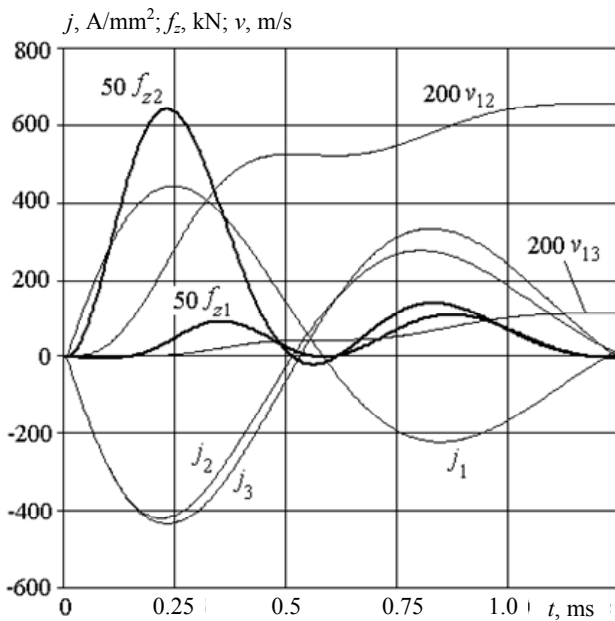


Fig. 4. Electromechanical characteristics of the LPIEC with armatures geometrical parameters $h_2^*=0.4$, $h_3^*=0.4$

In this LPIEC, the EDF f_{z1} is practically not effective on the inductor until the time 0.15 ms. As a result, the displacement of the inductor relative to the SA begins almost in 0.25 ms. The maximum value of these forces is observed in the second peak of repulsion and is only 1.85 kN. As a result, the inductor moves relative to the SA with a speed v_{13} , the maximum value of which is 0.56 m/s. The maximum speed of the MA relative to the SA v_{23} is 3.84 m/s.

LPIEC force and speed indicators. Let us consider influence of the geometrical parameters of the SA $h_2^* \in [0.3; 0.7]$ and the MA $h_3^* \in [0.3; 0.7]$ on the value of the EDF impulse $F_{zp} = \int f_{zp} dt$, where $p = 1, 2, 3$ are the indexes of the inductor, MA and SA.

The values of the EDF impulses acting on the inductor F_{z1} are much smaller than the values of the impulses acting on the MA F_{z2} and SA F_{z3} . The maximum values of the EDF impulse F_{z1} , acting on the inductor,

arise at geometrical parameters of armatures $h_3^*=0.4$ and $h_2^*=0.7$ (Fig. 5). The minimum values of F_{z1} arise when $h_3^*=0.7$ and $h_2^*=0.4$. The largest value of the EDF impulse F_{z1} at any height of the MA is realized for a SA with a parameter $h_3^*=0.4$.

The smallest values of the EDF impulse F_{z2} acting on the MA, on the contrary, arise for $h_3^*=0.4$ (the minimum value takes place for a high MA $h_2^*=0.7$). The greatest values of the EDF impulse F_{z2} occur at $h_2^*=0.42-0.45$ (the maximum value takes place at a high SA $h_3^*=0.7$).

The largest values of the EDF impulse F_{z3} , acting on the SA, arise for $h_3^*=0.4$ (the maximum value occurs for $h_2^*=0.7$). And the largest values of the EDF impulse F_{z3} take place when $h_2^*=0.4$ (the minimum value occurs for $h_3^*=0.7$).

Let us consider the influence of the geometric parameters of the SA $h_2^* \in [0.3; 0.7]$ and MA $h_3^* \in [0.3; 0.7]$ on the speed of the inductor and the MA, realized at the end of the operating process (Fig. 6).

The maximum value of the speed of the MA relative to the inductor V_{12} is realized with its minimum height $h_2^*=0.3$ and the maximum height of the SA $h_3^*=0.7$, and the minimum value of the speed of the MA relative to the inductor V_{12} is realized at its maximum height $h_2^*=0.7$ and the minimum height of the SA $h_3^*=0.3$.

In turn, the highest values of the speeds of the displacement of the inductor relative to the SA V_{13} occur at a relatively low SA $h_3^*=0.4$ (the maximum speed occurs at a high MA $h_2^*=0.7$). The lowest values of the speeds V_{13} are realized at $h_2^*=0.45$ (the minimum speed V_{13} occurs for high SA $h_3^*=0.7$).

Of greatest interest is the speed of the displacement of the MA relative to the SA V_{23} . As the calculations show, the highest speeds V_{23} the lowest MA $h_2^*=0.3$ develops, and the height of the SA does not affect it practically. However, with the increase in the height of the MA, the influence of the SA begins to affect. In this case, it is expedient to select the height of the SA with geometric parameters $h_3^* = 0.4-0.42$.

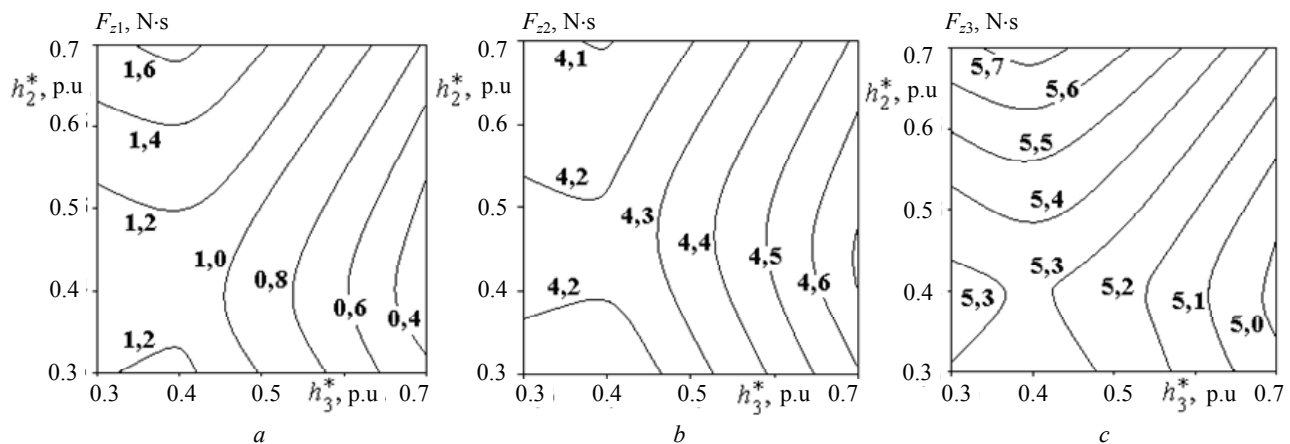


Fig. 5. Dependence of the EDF impulses acting on the inductor (a), MA (b) and SA (c) on the geometrical parameters h_2^* and h_3^*

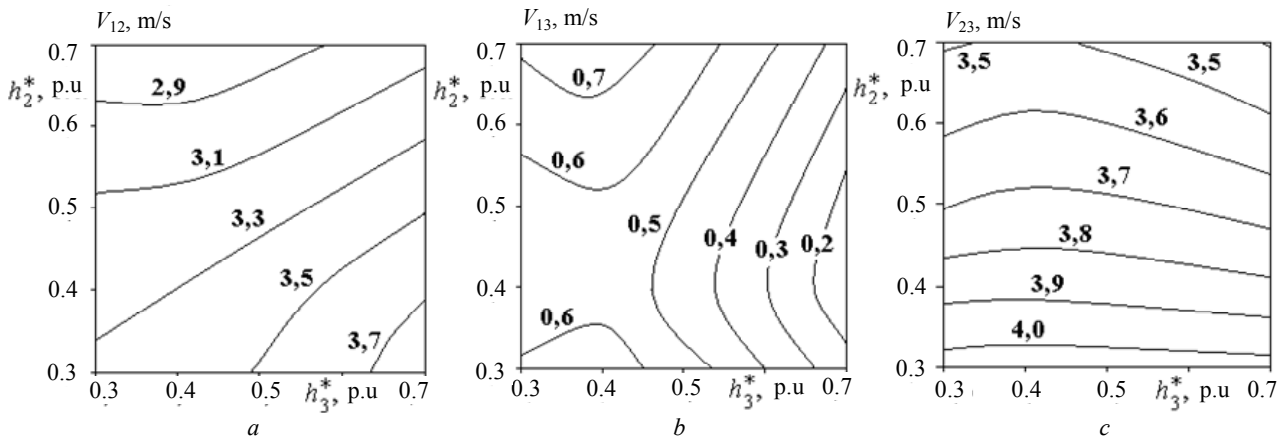


Fig. 6. Dependence of the speeds of the MA relative to the inductor (a), of the inductor relative to the SA (b) and the MA relative to the SA (c) on the geometrical parameters h_2^* and h_3^*

Effect of the mass of the actuating element on the LPIEC indicators. In order to more fully understand the electromechanical processes in the LPIEC, let us consider the effect of the mass of the actuating element m_e on its electromechanical indicators. Fig. 7 shows the dependencies of the indicators of the LPIEC having geometrical parameters of armatures $h_2^*=0.5$, $h_3^*=0.5$, on the mass of the actuating element. With an increase in the mass m_e , there is a significant decrease in the speed of displacement of the inductor relative to the SA V_{13} , which practically decreases to zero even at a mass $m_e=3$ kg. The speed of the MA relative to the inductor V_{12} with an increase in the mass of the actuating element from 0 to 5 kg decreases from 9.83 m/s to 0.9 m/s.

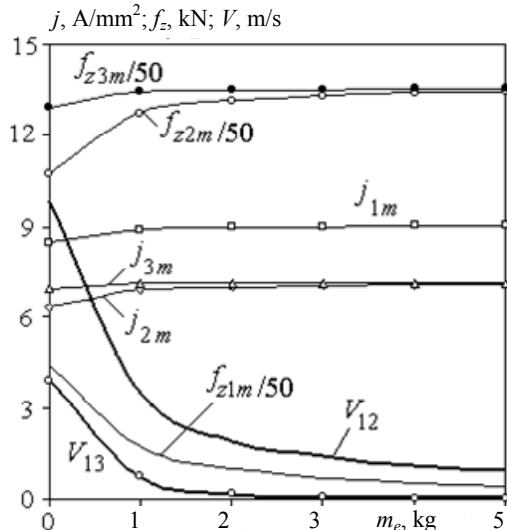


Fig. 7. Dependencies of the indicators of the LPIEC with parameters $h_2^*=0.5$, $h_3^*=0.5$ on the mass of the actuating element

Dependencies of the maximum EDF values acting on the active elements of the LPIEC, on the mass of the actuating element, have the following features. With increasing mass m_e , the maximum EDF values acting on the inductor f_{z1m} decrease and on the armatures increase. Moreover, the maximum EDFs acting on the MA f_{z2m} are smaller than the analogous forces acting on the SA f_{z3m} . However, as the mass of the actuating element increases, these forces tend to equalize. Obviously, with a fully retarded MA, these EDFs will be equal.

With an increase in mass m_e , there is an increase in currents both in the inductor and in the armatures, especially strongly in the interval 0 ... 1 kg. This can be explained by a stronger induction interaction of the inductor with armatures, which are in a strong magnetic coupling.

Conclusions.

1. A mathematical model is developed that describes the electromechanical processes of LPIEC with a movable inductor interacting with stationary and mobile electrically conductive armatures.

2. The effect of armatures heights on electromechanical processes of LPIEC was established. It is shown that at the initial moment of the operating process, the currents in the armatures have a polarity opposite to the inductor current.

3. It is shown that if the height of the SA is two times more than the height of the MA, then the EDF acts on the inductor at the initial instant of time, pressing it to the SA, and the displacement of the inductor begins with a delay of 0.35 ms. If the height of the MA is twice the height of the SA, then the EDFs act on the inductor at the initial instant of time, repelling it from the SA, and its movement begins with a delay of 0.1 ms. If the heights of the SA and the MA are equal, then until the time 0.15 ms the EDFs practically does not act on the inductor and the inductor moving relative to the SA begins with a delay of 0.25 ms.

4. The influence of the heights of the disk armatures on the values of the EDF impulses acting on the inductor and the armatures is established. The values of the EDF impulses acting on the inductor are much smaller than the EDF impulses acting on the armatures. Combinations of armatures heights are established, in which both the largest and the smallest impulses of the EDF act on them and on the inductor.

5. The effect of the geometric parameters of the SA and the MA on the speeds of the inductor and the MA is established. The highest speeds are developed by the lowest MA, and the height of the SA practically has no effect on them. However, with the increase in the height of the MA, the influence of the SA begins to affect. In this case, it is expedient to choose the height of the SA with a geometric parameter $h_3^*=0.4-0.42$.

6. It is shown that with an increase in the mass of the actuating element, the currents in the active elements of

the LPIEC increase and the speeds of the inductor and the MA decrease. In this case, the maximum values of the EDFs acting on the inductor reduce, and on the armatures increase. The maximum EDFs acting on the MA are less than similar forces acting on the SA.

REFERENCES

1. Balikci A., Zabar Z., Birenbaum L., Czarkowski D. Improved performance of linear induction launchers. *IEEE Transactions on Magnetics*, 2005, vol.41, no.1, pp. 171-175. doi: **10.1109/tmag.2004.839283**.
2. D.-K. Lim, D.-K. Woo, I.-W. Kim, D.-K. Shin, J.-S. Ro, T.-K. Chung, H.-K. Jung. Characteristic Analysis and Design of a Thomson Coil Actuator Using an Analytic Method and a Numerical Method. *IEEE Transactions on Magnetics*, 2013, vol.49, no.12, pp. 5749-5755. doi: **10.1109/tmag.2013.2272561**.
3. Tomashevsky D.N., Koshkin A.N. Modeling of linear impulse electric motors. *Russian Electrical Engineering*, 2006, no.1, pp. 24-27. (Rus).
4. Bolyukh V.F., Oleksenko S.V., Shchukin I.S. Comparative analysis of linear pulse electromechanical converters electromagnetic and induction types. *Technical Electrodynamics*, 2016, no.5, pp. 46-48. (Rus).
5. Young-woo Jeong, Seok-won Lee, Young-geun Kim, Hyun-wook Lee. High-speed AC circuit breaker and high-speed OCD. *22nd International Conference and Exhibition on Electricity Distribution (CIRED 2013)*, 2013, 10-13 June, Stockholm, Paper 608. doi: **10.1049/cp.2013.0834**.
6. Ivanov V.V., Pararin S.N., Nozdrin A.A. Semiautomatic installation of magnetic pulse compaction of powders. *Materialovedenie*, 2011, no.7, pp. 42-45. (Rus).
7. Ivashin V.V., Penchev V.P. Features of the dynamics of work and energy diagrams of pulsed electromagnetic drive with parallel and series connection of excitation windings. *Electrical engineering*, 2013, no.6, pp. 42-46. (Rus).
8. Bolyukh V.F., Luchuk V.F., Rassokha M.A., Shchukin I.S. High-efficiency impact electromechanical converter. *Russian electrical engineering*, 2011, vol.82, no.2, pp. 104-110. doi: **10.3103/s1068371211020027**.
9. Bolyukh V.F., Shchukin I.S. *Lineinye induktsionno-dinamicheskie preobrazovateli* [Linear induction-dynamic converters]. Saarbrücken, Germany, LAP Lambert Academic Publ., 2014. 496 p. (Rus).
10. Bissal A., Magnusson J., Engdahl G. Comparison of two ultra-fast actuator concept. *IEEE Transactions on Magnetics*, 2012, vol.48, no.11, pp. 3315-3318. doi: **10.1109/tmag.2012.2198447**.
11. Schneider Electric Industries SAS. *Electric switching device with ultra-fast actuating mechanism and hybrid switch comprising one such device*. Patent USA, no.8686814, 2014.
12. Bolyukh V.F., Shchukin I.S. The thermal state of an electromechanical induction converter with impact action in the cyclic operation mode. *Russian electrical engineering*, 2012, vol.83, no.10, pp. 571-576. doi: **10.3103/s1068371212100045**.

Received 05.01.2018

V.F. Bolyukh¹, Doctor of Technical Science, Professor,
A.I. Kocherga¹, Postgraduate Student,
I.S. Schukin², Candidate of Technical Science, Associate
Professor,

¹National Technical University «Kharkiv Polytechnic Institute»,
2, Kyrpychova Str., Kharkiv, 61002, Ukraine,
phone +380 57 7076427,

e-mail: vfbolyukh@gmail.com

²Firm Tetra, LTD,

2, Kyrpychova Str., Kharkiv, 61002, Ukraine,

phone +380 57 7076427,

e-mail: tech@tetra.kharkiv.com.ua

How to cite this article:

Bolyukh V.F., Kocherga A.I., Schukin I.S. Investigation of a linear pulse-induction electromechanical converter with different inductor power supply circuits. *Electrical engineering & electromechanics*, 2018, no.2, pp. 11-17. doi: **10.20998/2074-272X.2018.2.02**.